Longitudinal Exome-Scale Liquid Biopsy Monitoring of Evolving Therapeutic Resistance Mechanisms in Head and Neck Squamous Cell Carcinoma Patients Receiving Anti-PD-1 Therapy

Charles W. Abbott[1], Nikita Bedi[2], Jing Wang[1], Simo V. Zhang[1], Josette Northcott[1], Robin Li[1], Rachel Marty Pyke[1], Eric Levy[1], Rebecca Chernock[3], Mena Mansour[3], A. Dimitrios Colevas[2], John Lyle[1], John B. Sunwoo[2], Sean M. Boyle[1], Richard Chen[1]
[1]Personalis, Inc., Menlo Park, CA | [2]Stanford University, Stanford, CA | Washington University in St. Louis, St. Louis, MO.

#555

Contact:
charles.abbott@personalis.com

Background

Typical liquid biopsy panels capture a relatively small number of variants, and likely under-represent the heterogeneity of resistance in late-stage cancers. To address the challenges associated with identifying multiple concurrent heterogeneous resistance mechanisms in individual patients, we evaluated longitudinal whole exome sequencing of cell free DNA (cfDNA) and solid tumor biopsies from head and neck squamous cell carcinoma (HNSCC) patients that received anti-PD1 therapy. Using this approach, we identified evolving variant and pathway-level resistance mechanisms in cfDNA as a complement to tumor biopsy-derived information, and identified differences in putative neoantigens.
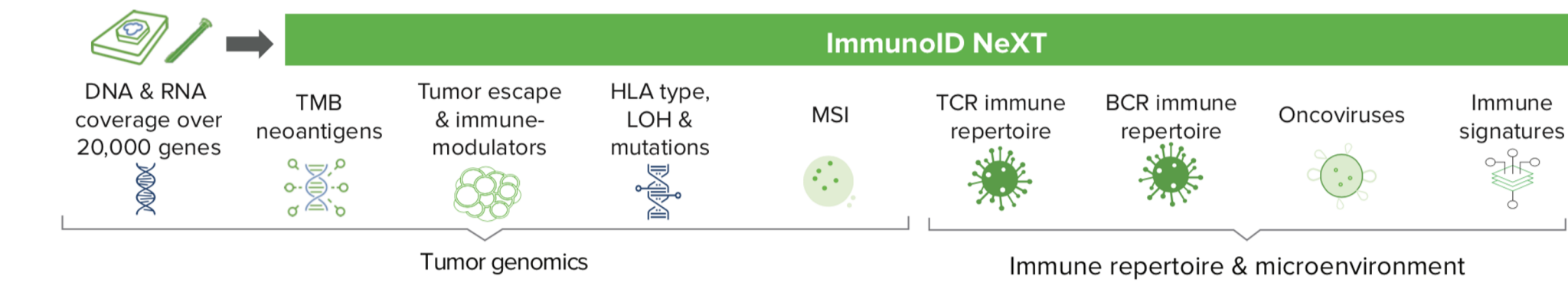
Methods

Cohort

Pre- and post-intervention matched tumor, normal and plasma samples were obtained from a cohort of 15 patients with HNSCC. Following baseline sample collection, all patients received a single dose of nivolumab. The primary tumor was then resected, approximately one month later when possible, or a second biopsy was collected where resection was impractical.

Solid tumor

Paired tumor and normal samples were profiled using ImmunoID NeXT™, an augmented exome/transcriptome platform and analysis pipeline which produces comprehensive tumor mutation information, gene expression profiling, neoantigen characterization including our composite neoantigen burden score NEOPS™, HLA typing and allele-specific LOH, TCR repertoire profiling, and tumor microenvironment profiling as outlined in the plot below.

Whole exome sequencing from plasma

Exome-scale cfDNA profiling of matched plasma samples was performed using the NeXT Liquid Biopsy™ platform. Sensitive variant detection across the exome was achieved using an enhanced exome assay and chemistry that augments difficult to sequence genomic regions yielding more uniform, high average depth coverage (2000X) across the exome, with boosted coverage (5000X) for 248 clinically relevant genes. To analyze the data we used tools which incorporate an error suppression model estimated from a panel of normal individual plasma samples, and ad hoc filters including a dedicated blacklist.
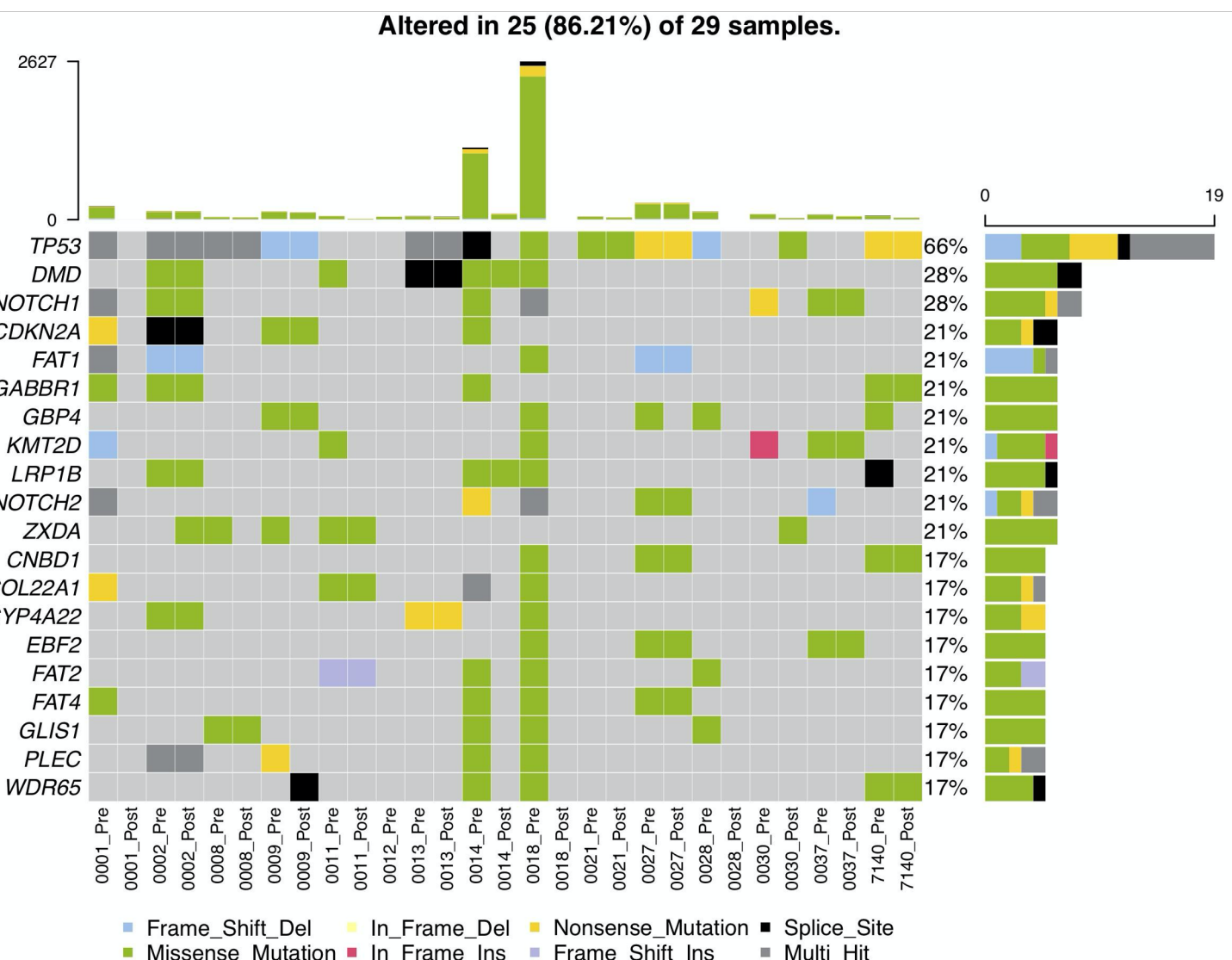
Results

Patient demographics

The demographics of the two groups of HNSCC subjects were similar. Baseline characteristics were summarized for each treatment group and presented as frequency distributions and/or summary statistics. Baseline data for all comparisons were those values recorded before immunotherapy, at the time of initial biopsy. Patient responses, as defined by RECIST criteria or histological assessment, were classified as either responder or non-responder. One patient stopped early due to biopsy proven metastatic disease. A second patient with early recurrence and metastatic disease received subsequent chemoradiation (Cisplatin and 66Gy). Demographic data was unavailable for one patient.

Characteristic	N	Overall, N = 14[1]	Non_responder, N = 8[1]	Responder, N = 6[1]	p-value[2]
Age	14	62.21 (13.66)	62.75 (16.68)	61.50 (9.71)	0.7
Sex	14				>0.9
F		6 (43%)	3 (38%)	3 (50%)	
M		8 (57%)	5 (62%)	3 (50%)	
Tumor site	14				0.5
Alveolar Ridge		2 (14%)	2 (25%)	0 (0%)	
Hard Palate		1 (7.1%)	0 (0%)	1 (17%)	
Maxillary Sinus		1 (7.1%)	1 (12%)	0 (0%)	
Oropharynx		1 (7.1%)	1 (12%)	0 (0%)	
Retromolar Trigone		1 (7.1%)	1 (12%)	0 (0%)	
Skin		4 (29%)	1 (12%)	3 (50%)	
Tongue		4 (29%)	2 (25%)	2 (33%)	
Stage	14				0.7
II		2 (14%)	1 (12%)	1 (17%)	
III		1 (7.1%)	0 (0%)	1 (17%)	
IV		11 (79%)	7 (88%)	4 (67%)	
p16 status	14				0.2
Negative		6 (43%)	5 (62%)	1 (17%)	
Positive		2 (14%)	1 (12%)	1 (17%)	
Unknown		6 (43%)	2 (25%)	4 (67%)	
Intervention	14				>0.9
Nivolumab		7 (50%)	4 (50%)	3 (50%)	
Nivolumab_resection		7 (50%)	4 (50%)	3 (50%)	

[1] Mean (SD); n (%)
[2] Wilcoxon rank sum test; Fisher's exact test

Tumor mutational landscape

Altered in 25 (86.21%) of 29 samples.
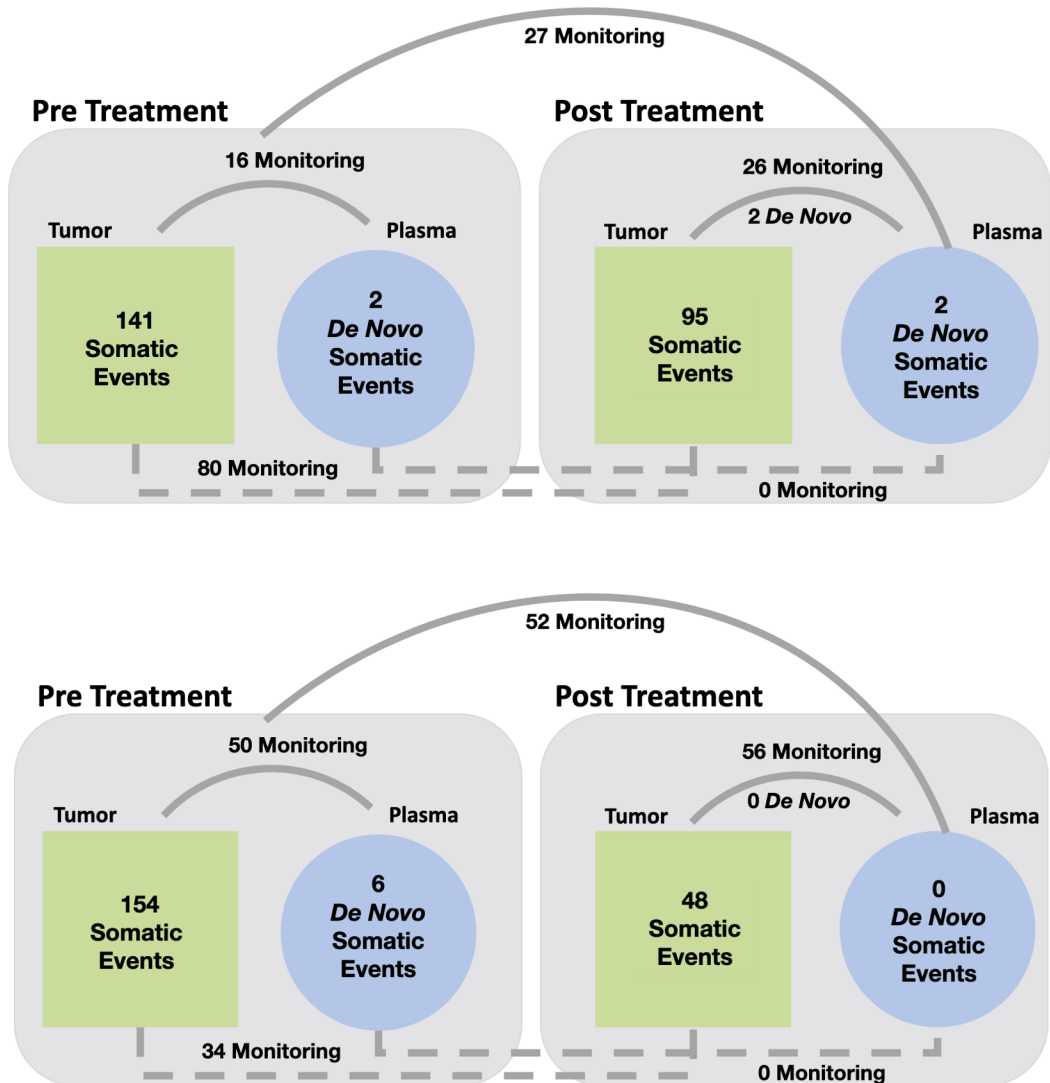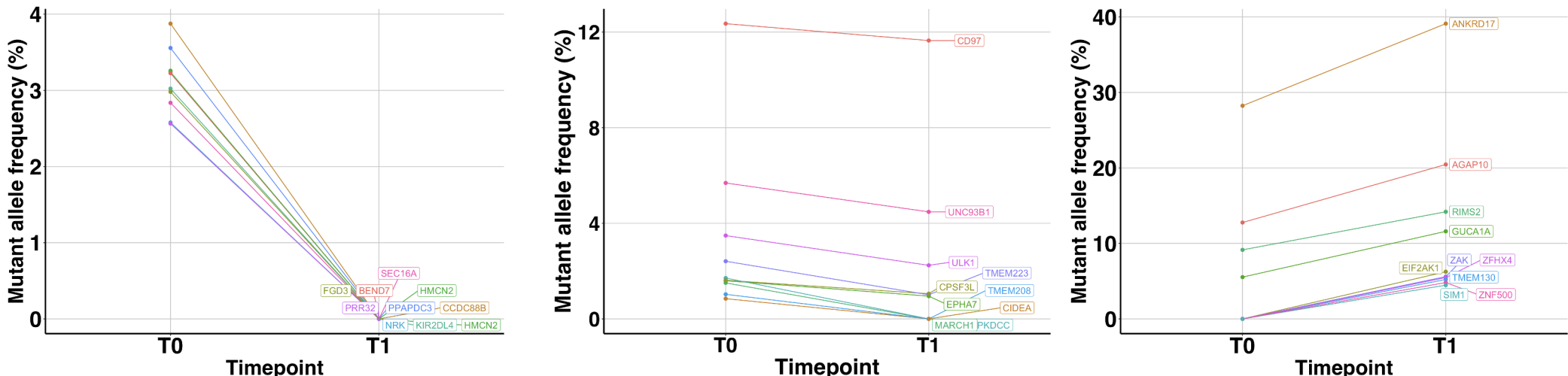

The solid tumor mutational landscape in patients pre- and post-intervention was investigated. The most commonly identified mutation occurred in TP53, which was identified in 80% of patients. A clear reduction in mutational burden was observed in patients that responded to therapy (example: patient 0001 and 0018). Similarly, neoantigen burden is significantly reduced following intervention (Wilcoxon signed rank; P = 0.02). Pretreatment intratumor heterogeneity (ITH) was elevated in non-responding patients (P = 0.013).

Concordant somatic events in tumor and plasma

Liquid biopsy is particularly attractive in cases where multiple biopsies are needed for longitudinal monitoring of disease progression. At right, we explore the concordance observed between somatic events observed in solid tumor, and those detected in plasma in a pre/post therapeutic intervention paradigm. Strong concordance was observed in all patients, and an average of 120 ctDNA-based variants were detected in the cohort. ITH was found to positively correlate with de novo somatic events detected in plasma (Spearman's rho = 0.75, P = 0.01), suggesting that paired liquid biopsy may provide critical information that would have otherwise been missed in a single-lesion biopsy approach, particularly in heterogeneous malignancies. Indeed, amongst the variants detected only in plasma we found hallmark oncogenes including FAT1 and ROS1, both of which exert significant influence on the trajectory of disease development and therapeutic response.
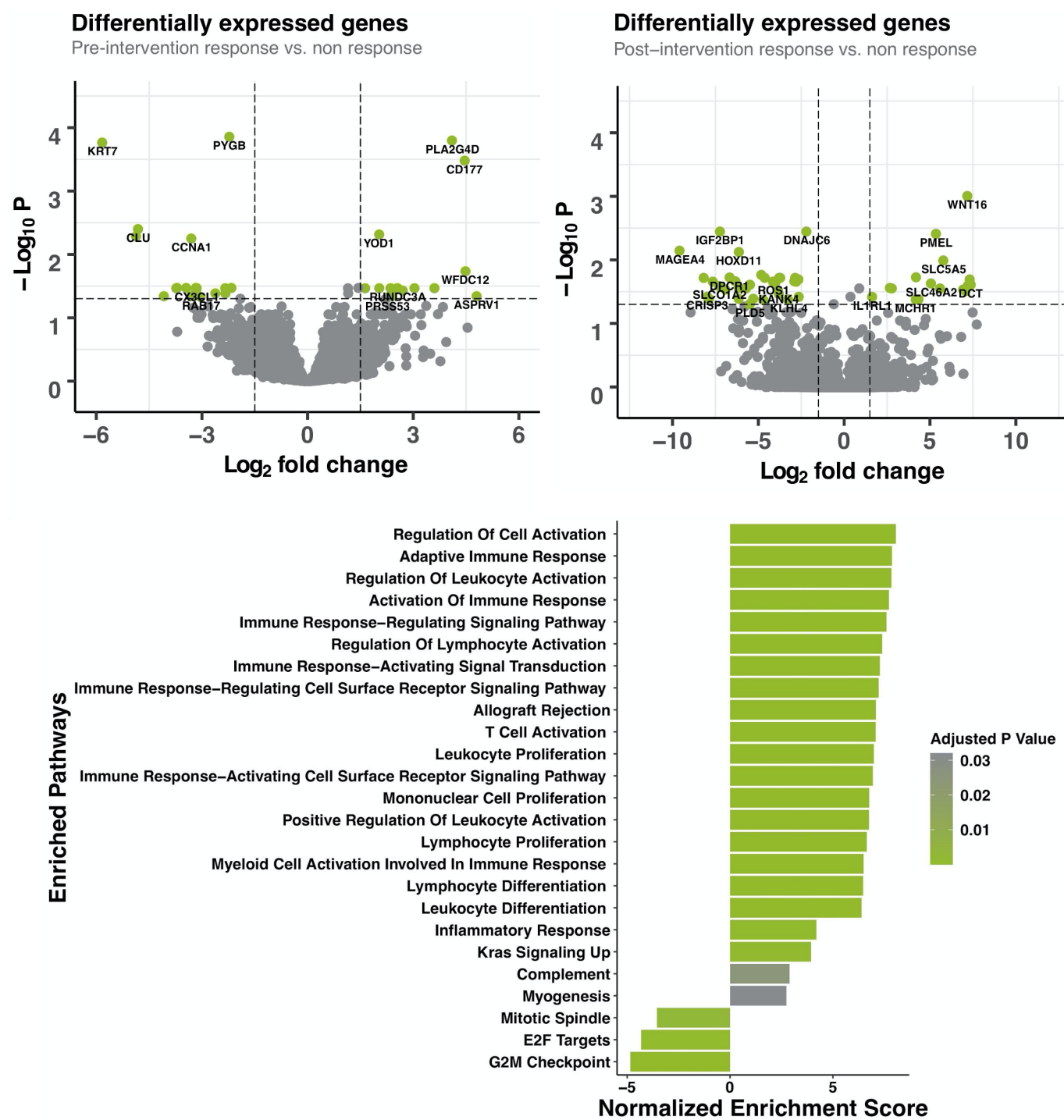

cfDNA VAF changes in response to intervention

Large, clustered shifts in variant allele frequency (VAF) were detected in all patients despite the relatively short period of time between pre- and post-intervention timepoints. When considering clusters of decreasing VAF genes in two responder patients (left and center) we find reduction in genes such as CD97 and KIR2DL4. Review of genes with increasing VAFs in a non-responding patient (right) revealed an increase in ANKRD17, part of the MMR system, possibly reflecting one mechanism of immune evasion and reduced therapeutic efficacy in this patient.

Transcriptomic analysis

Next, we identified transcriptomic profiles associated with response both pre- and post-intervention. Amongst other expression changes, a significant reduction in ROS1 expression was detected post-intervention in responding patients. Pathway analysis was conducted (Parametric Analysis of Gene Set Enrichment) to identify pathway level changes associated with therapeutic intervention. Notably, post-intervention patients were significantly enriched relative to pre-intervention for pathways involved in immune response including antigen receptor mediated signaling, T cell activation and regulation of lymphocyte activation. These changes are largely driven by transcriptional activation in responding patients.

Conclusions

Exome-wide somatic events were reliably detected in cfDNA, providing additional potential biomarkers to complement those identified in solid tumor. As we increase our cohort size, we expect that identification of biomarkers from both exome scale tissue biopsy and cfDNA will provide a more comprehensive view into therapeutic response and resistance mechanisms in HNSCC patients missed with either single-lesion biopsies or typical liquid biopsy panels.